Archives of Mechanics • Archiwum Mechaniki Stosowanej • 26, 3, pp. 355–367, Warszawa 1974

Skimming of molecular beams from diverging non-equilibrium gas jets

U. BOSSEL (GÖTTINGEN)

THE FORMATION of molecular beams by skimming techniques has become accepted in all domains, where well-defined monoenergetic flows of atoms or molecules are needed. Common to all applications is the desire to maximize the beam particle density, or flux, without sacrifice of the free molecular behaviour of the flow. Obviously, these requirements call for compromizes. Additional constraints on the beam properties are imposed by the diverging nature and by the local temperature anisotropy of the highly rarefied free jet expansions from which beam molecules are normally extracted. In this paper the equations for the density of molecular beams generated under the conditions indicated are developed and numerical solutions are presented. Experimental evidence appears to verify the analytical treatment of the problem.

Metodę uzyskiwania wiązek molekularnych za pomocą tzw. "skimmerów" — odpowiednio ukształtowanych przesłon — stosuje się powszechnie wszędzie tam, gdzie zachodzi potrzeba posługiwania się ściśle określonymi, monoenergetycznymi przepływami atomów lub cząsteczek. We wszystkich zastosowaniach chodzi nam o zwiększenie gęstości cząsteczek w wiązce i o równoczesne zachowanie swobodno-molekularnego charakteru samego przepływu. Już te wymagania są częściowo sprzeczne. Dalsze ograniczenia własności wiązki wynikają z rozbieżnego charakteru wysoce rozrzedzonego strumienia gazu, z którego pobierana jest badana wiązka, jak również lokalnej anizotropii temperatury w tym strumieniu. W pracy wyprowadzono równania dla gęstości wiązek molekularnych, utworzonych w opisany sposób, oraz przedstawiono rozwiązania numeryczne tych równań. Badania eksperymentalne wydają się potwierdzać wyniki rozważań analitycznych.

Метод получения молекулярных пучков при помощи т. наз. "скиммеров" — соответственно формированных диафрагм — применяется везде там, где надо пользоваться точно определенными, моноэнергетическими течениями атомов или молекул. Во всех применениях идет дело об увеличении плотности молекул в пучке и об одновременном сохранении свободно-молекулярного характера самого течения. Уже эти требования частично противоречивы. Дальнейшие ограничения свойств пучка вытекают из расходящего характера сильно разреженного потока газа, из которого получается исследуемый пучок, как тоже из локальной анизотропии температуры в этом потоке. В работе выведены уравнения для плотности молекулярных пучков, образованных описанным способом, и представлены численные решения этих уравнений. Экспериментальные исследования кажутся подтверждать результаты аналитических рассуждений.

List of symbols

(in CGS-units, unless otherwise specified)

A, B, C coefficient of a quadratic equation, Eq. (11),
A_S skimmer area,
b modified speed ratio, $b \equiv S_{\parallel} \varepsilon \cos\theta$, Eq. (5),
c most probable speed of a molecule, $c \equiv (2kT/m)^{1/2}$,
D diameter,
$D(b)$ density function, Eq. (5),
$f(v, \theta)$ velocity distribution function, Eq. (2),
k Boltzmann's constant,

l length, see Fig. 2,
m molecular mass,
N number density within molecular beam,
n number density within free jet flow,
p pressure,
R_F radius of spherical quitting surface,
r radius,
S molecular speed ratio, Eq. (5),
$\mathbf{s}$ streamline vector,
T temperature,
$\mathbf{U}$ hydrodynamic velocity,
v molecular velocity,
x, y, z orthogonal coordinate system,
α azimuthal angle,
β angle between molecule trajectory and beam axis,
γ ratio of the specific heats,
δ angle of flow divergence,
ε dimensionless parameter, Eq. (5),
η azimuthal angle,
θ angle between molecule trajectory and streamline,
ξ parameter, Eq. (10),
ϱ dimensionless radius, $\varrho \equiv r/r_S$,
τ temperature ratio, $\tau \equiv T_{||}/T_{\perp}$,
Φ constant given by Ref. [7],
φ dimensionless angle, $\varphi \equiv \alpha/\pi$,
ω solid angle.

Subscripts

D refers to detector,
S refers to skimmer,
R refers to quitting surface,
is refers to isentropic conditions,
o refers to stagnation conditions,
$\perp$ perpendicular to a streamline,
$||$ parallel to a streamline.

1. Introduction

THE PROPERTIES of molecular beams generated by skimming the core of a diverging rarefied hypersonic gas flow have been the subject of repeated treatment. The early work by PARKER *et al.* [1] describes the beam formation for uniform equilibrium flows at the skimmer. Later, when free jet expansions became widely used in beam experiments, ANDERSON and FENN [2], FRENCH [3], KNUTH *et al.* [4] and HAGENA and MORTON [5] suggested refined analyses accounting for flow divergence at the skimmer and anisotropic conditions in the flow field. Nevertheless, all these analyses suffer from a number of simplifications which in the light of this work may effect the numerical results to a much greater extent than previously assumed. The first hint that detailed account must be taken of a variety of parameters was offered by LEROY and GOVERS [6]. The present study should be considered a refined extension of their work. It can be shown that all previously proposed descriptions of the beam formation process are contained in the current analysis.

2. Theory

The formation of molecular beams is schematically illustrated in Fig. 1. For an oven beam the molecules escape from a source region at rest. By contrast, for the nozzle beam

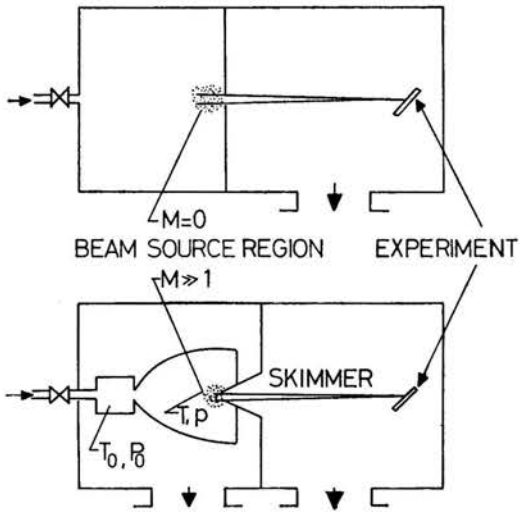

FIG. 1. Scheme of oven and nozzle beam system.

the gas in this region is moving towards the skimmer slit with a mean velocity **U** resulting from expansion of the medium from high pressures into vacuum.

The details of the process of beam formation are shown in Fig. 2. Unless otherwise specified, the free expansion of the gas is assumed to follow the isentropic relations given

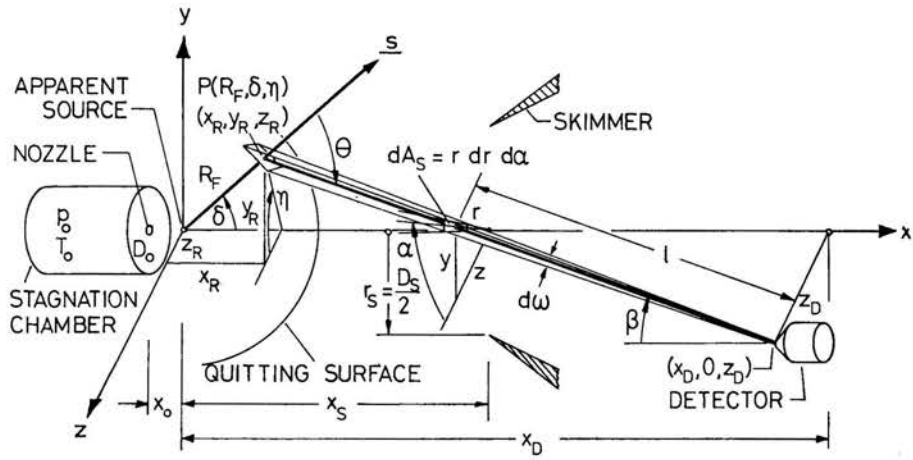

FIG. 2. Scheme of beam formation.

by ASHKENAS and SHERMAN [7] in a quasi-spherical source flow up to a quitting surface of radius R_F, where collisions between molecules abruptly cease to occur and a free molecule flow pattern exists from there on.

Molecules therefore "radiate" from the quitting surface. From a given detection point $(x_D, 0, z_D)$, an elementary area of the quitting surface can be seen through the "window" $dA'_S = r dr d\alpha \cos\beta$ in the skimmer plane. The solid angle pertinent to this problem is then defined by $d\omega = dA'_S/l^2 = r dr d\alpha \cos^3\beta/(x_D - x_S)^2$. It intercepts an area of the quitting surface centered about a streamline **s** which forms an angle θ with the line of sight between point $P(R_F, \delta, \eta)$ and the detection point $(x_D, 0, z_D)$. The angle between the streamline **s** and the main axis of the system is denoted by δ, the azimuthal angle by η. We can therefore immediately evaluate the contribution of this area element to the number density at the detector,

$$(1)\quad dN(x_D, 0, z_D) = n(R_F, \delta, \eta) f(v,\theta) d^3v = n(R_F, 0, 0)\cos^2\left(\frac{\pi\delta}{2\Phi}\right) f(v, \theta) v^2 dv\, d\omega$$

$$= n(R_F, 0, 0)\cos^2\left(\frac{\pi\delta}{2\Phi}\right) f(v, \theta) v^2 dv \cdot \frac{r\, dr\, d\alpha}{(x_D - x_S)^2} \cos^3\beta .$$

Here, the off-axis density variation given in reference [7] was introduced. The angle β denotes the directional difference between the beam axis and the line of sight. Note that the apparent source of the free jet flow is taken as the natural origin of molecules in this analytical treatment.

The distribution function $f(v, \theta)$ is assumed to be ellipsoidal to account for anisotropy of the molecular motion at the quitting location. We use the form

$$(2)\qquad f(v,\theta) = \pi^{-3/2} c_\perp^{-2} c_{||}^{-1} \exp\left[-\frac{v_\perp^2}{c_\perp^2}\right] \exp\left[-\frac{(v_{||} - U)^2}{c_{||}^2}\right],$$

where $v_\perp = v\sin\theta$ and $v_{||} = v\cos\theta$ denote the two components of the molecular velocity normal and parallel to the direction of mean mass propagation along the streamline **s**,

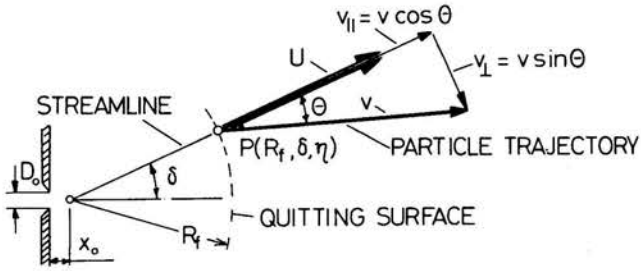

FIG. 3. Velocity vector diagram.

as shown in Fig. 3. The quantities $c_\perp = (2kT_\perp/m)^{1/2}$ and $c_{||} = (2kT_{||}/m)^{1/2}$ symbolize the most probable random molecular speeds in the two selected directions.

The integration of the Eq. (1) can then be attempted. We formally obtain:

$$(3)\quad N(x_D, 0, z_D) = \frac{n(R_F, 0, 0)}{\pi^{3/2} c_{||} c_\perp^2} \frac{1}{(x_D - x_S)^2} \int_0^{2\pi} d\alpha \int_0^{r_S} r\, dr \cos^3\beta \cos^2\left(\frac{\pi\delta}{2\Phi}\right) \times$$

$$\times \int_0^\infty \exp\left[-\frac{v^2 \sin^2\theta}{c_\perp^2}\right] \exp\left[-\frac{(v\cos\theta - U)^2}{c_{||}^2}\right] v^2 dv ,$$

where δ, β and θ depend on a variety of geometric parameters, as well as, on the integration variables r and α itself. The integration in the speed domain can be performed with little difficulty. Because of the complexity of the geometric relations between (δ, β, θ) and (r, α), the remaining integral must be solved numerically if simplifications are to be excluded. We then obtain in non-dimensionalized form:

$$N(x_D, 0, z_D) = \frac{1}{2} n(R_F, 0, 0) \cdot \tau \left(\frac{r_S}{x_D - x_S}\right)^2 \int_0^1 d\varphi \int_0^1 \varrho d\varrho \cos^3\beta \cos^2\left(\frac{\pi\delta}{2\Phi}\right) \times \tag{4}$$

$$\times \varepsilon^3 \exp[-S_{||}^2(1-\varepsilon^2\cos^2\theta)] D(b),$$

where

$$\begin{aligned} \varphi &\equiv \alpha/\pi, \\ \varrho &\equiv r/r_S, \\ S_{||} &\equiv U/c^{||}, \\ \tau &\equiv T^{||}/T^{\perp} = (c_{||}/c_{\perp})^2, \\ \varepsilon &\equiv (\tau\sin^2\theta + \cos^2\theta)^{-1/2}, \\ b &\equiv S_{||}\,\varepsilon\cos\theta, \end{aligned} \tag{5}$$

and $D(b) \equiv 2\pi^{-1/2} b \exp(-b^2) + (2b^2+1)\,[1+\mathrm{erf}(b)]$.

The integral, Eq. (4), is extremely sensitive to even small changes of ε and θ. Taking anything but the accurate geometric relationships between (δ, β, θ) and other system parameters might lead to significant departures of the approximate analysis from the "exact" solution. The geometric relations will therefore be listed. We obtain

$$\cos\delta = x_R/R_F, \tag{6}$$

$$\cos\beta = \frac{x_D - x_S}{l} = \frac{x_D - x_S}{[(x_D-x_S)+y^2+(z_D-z)^2]^{1/2}}, \tag{7}$$

and

$$\cos\theta = \frac{x_R(x_D-x_R) - y_R^2 + z_R(z_D-z_R)}{(x_R^2+y_R^2+z_R^2)^{1/2}[(x_D-x_R)^2+y_R^2+(z_D-z_R)^2]^{1/2}}. \tag{8}$$

The Cartesian coordinates x_R, y_R and z_R of the point $P(R_F, \delta, \eta)$ are defined by the following set of equations:

$$x_R = x_D - \xi(x_D - x_S), \quad y_R = y\left[\frac{x_D - x_R}{x_D - x_S}\right] \quad \text{and}$$

$$z_R = z\left[\frac{x_D - x_R}{x_D - x_S}\right] - z_D\left[\frac{x_D - x_R}{x_D - x_S}\right]. \tag{9}$$

Here, ξ is the negative root of a quadratic expression:

$$\xi = \frac{B - (B^2 - AC)^{1/2}}{A}, \tag{10}$$

where

$$\begin{aligned} A &\equiv (x_D - x_S)^2 + y^2 + (z_D - z)^2, \\ B &\equiv x_D(x_D - x_S) + z_D(z_D - z) \quad \text{and} \\ C &\equiv x_D^2 + z_D^2 - R_F^2. \end{aligned} \tag{11}$$

The dummy variables (y, z) are related to the integration variables (r, α) by

$$y = r\sin\alpha \quad \text{and} \quad z = r\cos\alpha,$$

with the restriction $0 \leqslant r \leqslant r_S$ — i.e., within the geometric limits of the skimmer aperture A_S over which the integration is performed.

3. Analytical results

The usefulness of the analysis presented will now be examined by a parametric variation of the most important quantities. To facilitate understanding of the results, a standard geometry has been chosen consisting of a nozzle diameter $D_0 = 1.0\,\text{mm}$, a virtual source-skimmer distance $x_S = 100\,\text{mm}$, a virtual source-detector distance $x_D = 200\,\text{mm}$ and a skimmer diameter $D_S = 4.0\,\text{mm}$. Unless otherwise specified, the computations are valid for this system of geometries and for helium as beam gas.

Figure 4 displays the off-axis beam density profiles, normalized to unity on the beam axis, for various detector locations x_D as a function of the divergence angle δ. It seems that

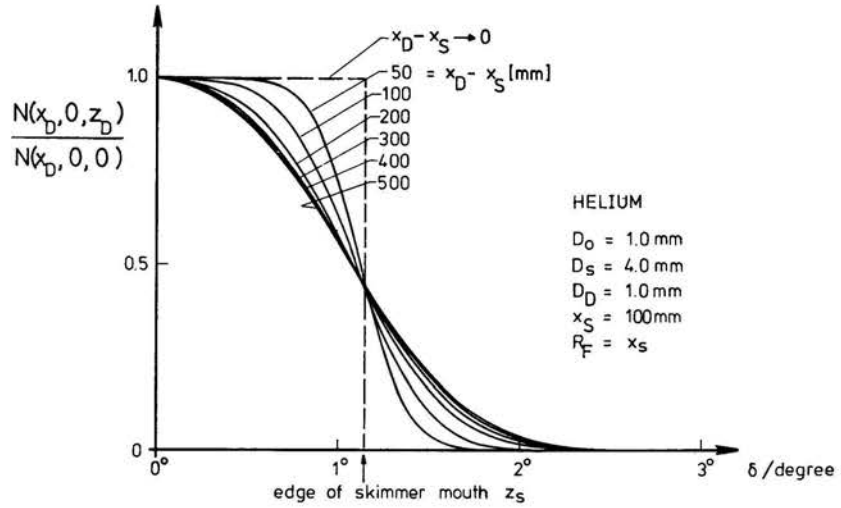

FIG. 4. Normalized beam density profile as a function of the divergence angle δ for different detector-skimmer distances.

self-similar density profiles are obtained only as x_D tends to infinity. For finite virtual source-detector distances, no universal profile can be specified. The details of the system geometry dominate at small values of x_D and quasi-rectangular profiles are obtained in analogy to the laws of optics. This finding suggests that the exact analysis should be considered when flow properties are extracted from molecular beam profiles.

The influence of the skimmer diameter D_S is illustrated in Fig. 5. Increasing the size of the aperture will initially lead to an increase of the number density on the beam axis. But for large values of D_S, only a widening of the density profile is predicted. The random spread of molecules at high speed ratios is so small that only a negligible fraction of molecules can reach the beam center from diverging streamlines.

The on-axis density is compared to predictions by the PARKER [1] and HAGENA-MORTON [5] analyses. Both theories agree with the present work at small divergence angles — i.e., for small D_S — but, whereas Parker's analysis [1] predicts an unlimited increase of $N(x_D, 0, 0)$ with D_S, the Hagena-Morton [5] study yields an upper limit for the center line density which is still considerably higher than the limit obtained in the present investigation.

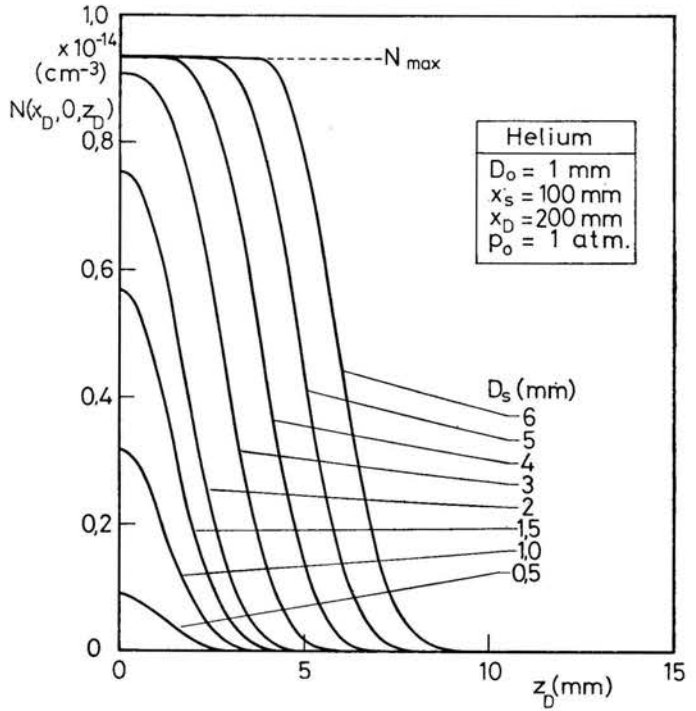

FIG. 5. Beam density profiles for different skimmer diameters.

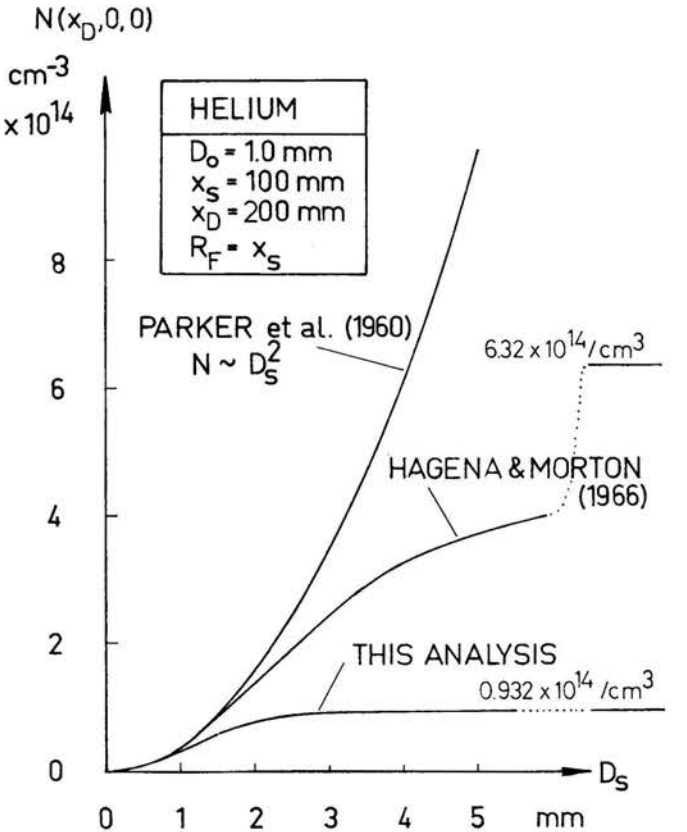

FIG. 6. Ideal center line beam densities as a function of the skimmer diameter. Comparison of different analyses.

Moreover, here the maximum density is obtained for much smaller skimmer diameters than in Ref. [5]. This result appears to be of significance to molecular beam experimenters.

The location of the quitting surface R_F scaled by the nozzle diameter D_0 again has a pronounced effect on the density profile, as illustrated in Fig. 7. With decreasing R_F/D_0 the profiles become increasingly rectangular. Interestingly enough, this profile variation does not, as shown in Fig. 8, effect the center line density to a significant extent.

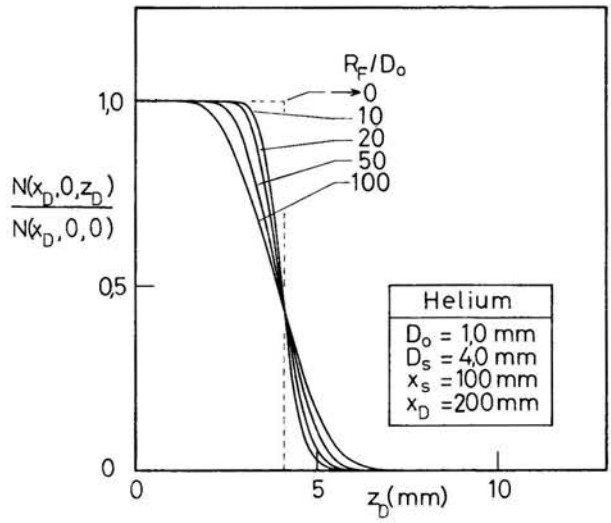

FIG. 7. Beam density profiles for different quitting surface radii.

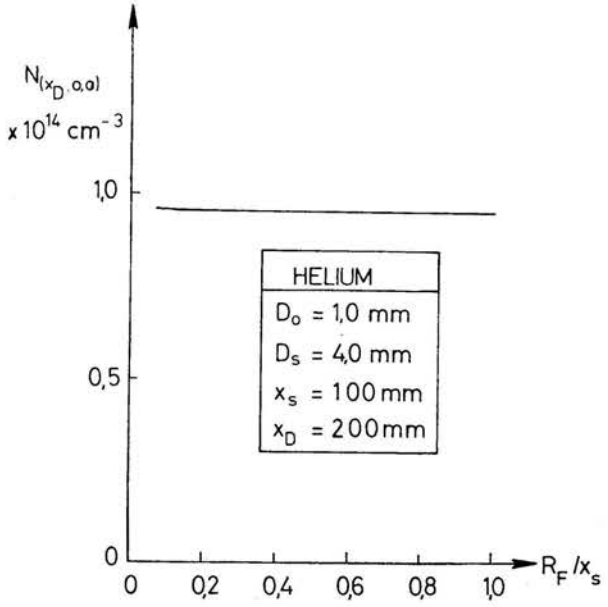

FIG. 8. Center line beam density as a function of the quitting surface locations.

The variation of the perpendicular temperature $T_\perp$ scaled by the isentropic value T_{is} for $R_F = x_S$ also yields density profiles of near-rectangular shapes for $T_\perp/T_{is} \to 0$ and of Gaussian character for $T_\perp/T_{is} \gg 1$, as illustrated in Fig. 9. But, whereas the variation of R_F/D_0 did not significantly affect the center line density of the beam, the temperature variation does, as seen in Fig. 10.

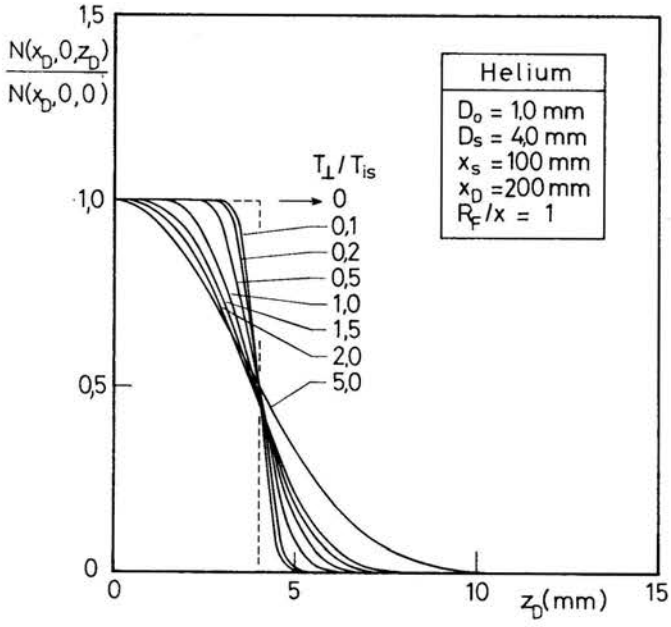

FIG. 9. Beam density profiles for different perpendicular temperatures.

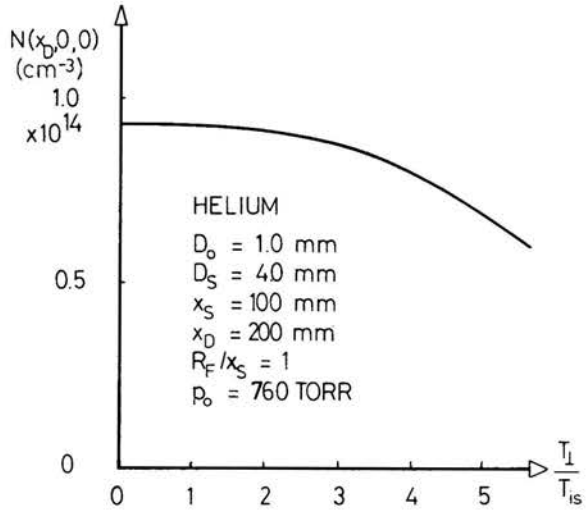

FIG. 10. Center line beam density as a function of the perpendicular temperature.

The peculiar temperat ureparallel to the streaming motion of the gas has hardly any effect on the beam properties studied. A graphic display of the parametric variation of $T_{||}/T_{1s}$ is therefore omitted.

Finally, in the light of the polytropic behaviour of many gases during a rapid expansion process, the ratio γ of the specific heats is varied between limits of 7/5 and 5/3 for the ideal diatomic and monatomic gas, respectively. The polytropic description of a rapid expansion

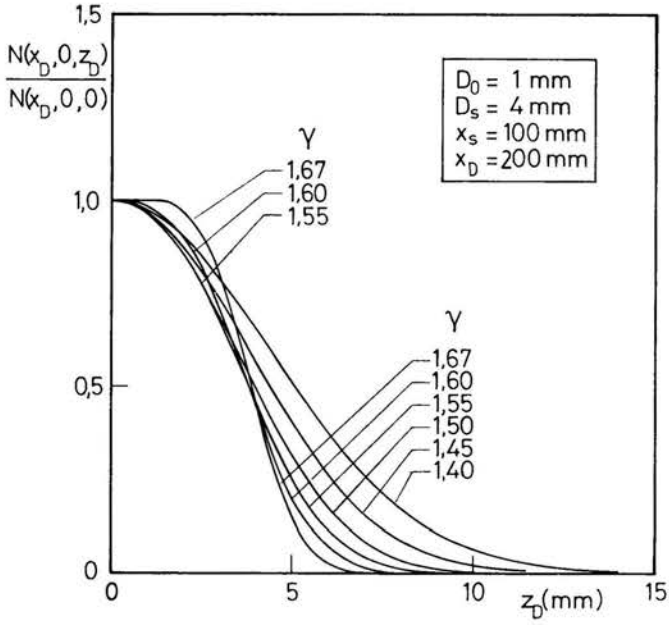

FIG. 11. Beam density profiles for polytropic expansions.

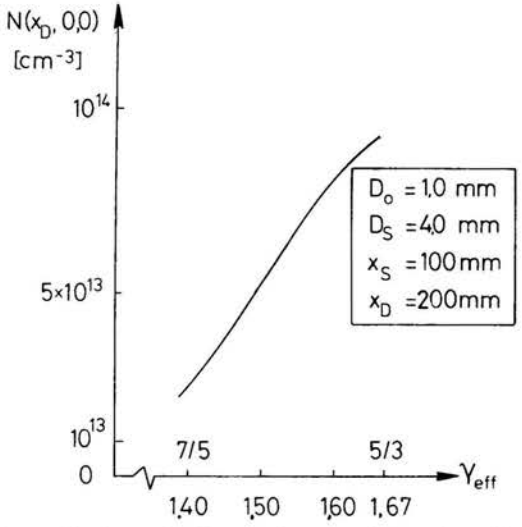

FIG. 12. Center line beam density as a function of the polytropic exponent.

of molecular gases into vacuum appears to be useful to describe the incomplete conversion of rotational into translational energy.

Figures 11 and 12 show the effects of polytropic behaviour on the beam profiles and the center line density, respectively. Rotationally relaxing gases (e.g. hydrogen) yield higher densities, or intensities, near the beam axis than those for which the effect is less pronounced under typical experimental conditions (e.g. nitrogen).

4. Experimental verification

A few experimental results taken from an earlier investigation [8] may serve to illustrate the usefulness of the analysis presented. In this work, all systematic parameters were similar to those analytically examined previously.

For helium, the comparison of experimental results is rather good, Fig. 13, even if the quitting surface is placed at the skimmer mouth. The match of the full width at half maximum to a Gaussian profile does not agree well with the experimental data and, moreover,

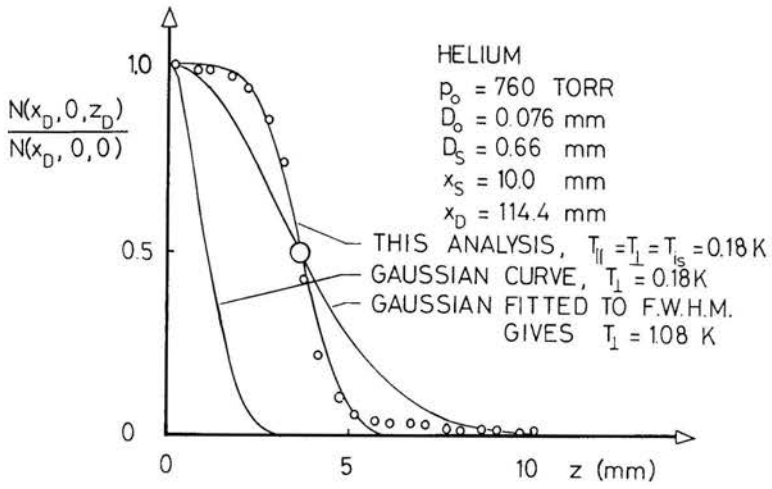

FIG. 13. Comparison of measured helium data with the "exact" and approximate analyses.

would have required an unreasonable temperature $T_{\perp}$ to complete the fit. The purely Gaussian curve for the temperature used in the analysis is, on the other hand, much narrower than the profile observed, indicating that both the random molecular motion and the divergence of stream lines must be accounted for in beam profile predictions.

The experiments with nitrogen, Fig. 14, yield results which can be compared neither to the ideal diatomic nor to the monatomic density profiles, but rather follow a polytropic trend. An effective γ of 1.52 was found to give the best fit to a polytropic profile, as illustrated in Fig. 15. This means that, roughly speaking, 30% of the energy originally contained in the rotational motion of the molecules has not been converted into translation during the rapid expansion process.

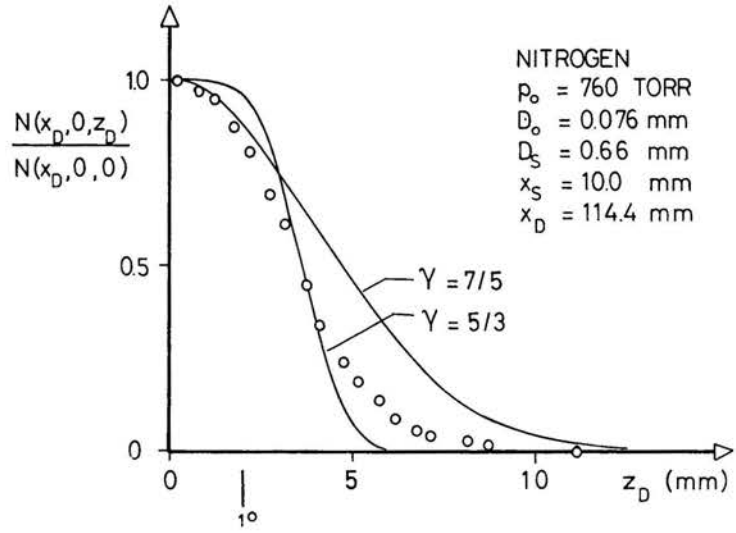

FIG. 14. Comparison of measured nitrogen data with the "exact" analysis.

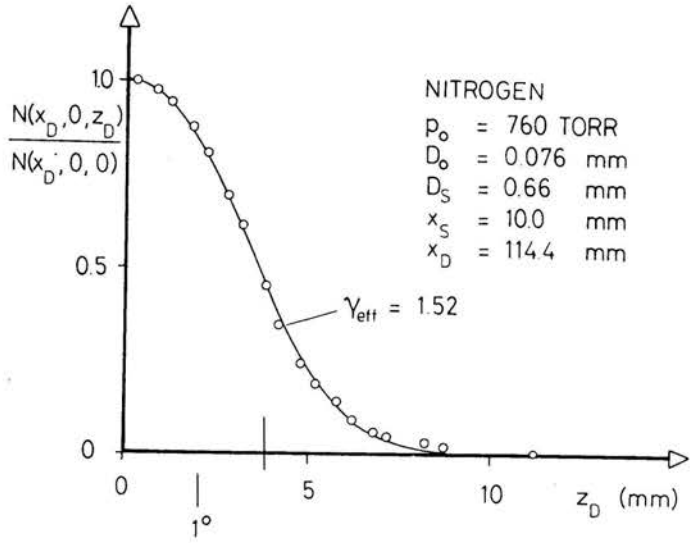

FIG. 15. Polytropic density profile fitted to nitrogen data.

5. Summary and conclusions

The presented "exact" analysis of the process of nozzle beam formation confirms existing analyses where approximations are allowed, but provides new evidence in areas where previous work was based on too many intuitive arguments. Although this work is by no means considered to be free of restrictive assumptions and simplified models, it may serve to warn experimentalists in their effort to extract flow properties from beam data using

simplified theories for data interpretation and analysis. Nevertheless, if undesired phenomena of skimmer interference and scattering attenuation can be minimized, or accounted for, then some flow properties can be measured by comparing beam profile data to a sophisticated analysis.

Reference

1. H. M. PARKER, A. R. KUHLTHAU, R. ZAPATA, J. E. SCOTT, *The application of supersonic beam sources to low-density, high-velocity experimentation*, RGD (F. M. DEVIENNE, Ed.), Pergamon Press, 69–79, London 1960.
2. J. B. ANDERSON, J. B. FENN, *Velocity distribution in molecular beams from nozzle sources*, Phys. Fluids, **8**, 780–787, 1965.
3. J. B. FRENCH, *Molecular beams for rarefied gasdynamic research*, AGARDograph, 112, 1966.
4. E. L. KNUTH, N. M. KULUVA, J. P. CALLINAN, *Densities and speeds in an arc-heated supersonic argon beam*, Entropie, **18**, 38–46, 1967.
5. O. F. HAGENA, H. S. MORTON, Jr., *Analysis of intensity and speed distribution of a molecular beam from a nozzle source*, RGD (C. L. BRUNDIN, Ed.), Academic Press, **2**, 1369–1384, New York 1967.
6. R. L. LEROY, T. R. GOVERS, *Ideal intensities of supersonic molecular beams*, Can. J. Chem., **48**, 1743–1747, 1970.
7. H. ASHKENAS, F. S. SHERMAN, *The structure and utilization of free jets in low density wind tunnels*, RGD (J. H. de LEEUW, Ed.), Academic Press, **2**, 84–105, New York 1966.
8. U. BOSSEL, R. DAVID, F. FAUBEL, K. WINKELMANN, *Free jet temperature extraction from molecular beam profiles*, RGD (K. KARAMCHETI, Ed.), Academic Press, New York, to be published).

DFVLR-INSTITUT FÜR DYNAMIK VERDÜNNTER GASE,
GÖTTINGEN, F.R.G.